

## Thermal efficiencies of NiTiCu shape memory alloys

F.J. Gil\*, J.A. Planell

*Dept. Ciencia de los Materiales e Ingeniería Metalúrgica ETSEIB, Universidad Politècnica Catalunya,  
Av. Diagonal 647, 08028 Barcelona, Spain*

Received 4 June 1998; received in revised form 13 October 1998; accepted 18 November 1998

### Abstract

Thermal efficiencies were calculated based on an ideal shape-memory-effect heat-engine cycle. It was found that the addition of copper in the NiTi shape-memory alloy provides an important increase of the thermal efficiency with the highest temperature transformation range. Thermal efficiency values obtained range from 4.7 to 5.3% and Carnot efficiencies were around 25%. These efficiencies have been evaluated by means of calorimetric techniques and mechanical tests for five NiTiCu shape-memory alloys. © 1999 Elsevier Science B.V. All rights reserved.

*Keywords:* Thermal efficiency; Shape-memory alloys; NiTiCu; Calorimetry

### 1. Introduction

The shape-memory effect, whereby a material will revert to its original shape after large deformations by heating, makes these materials interesting working media for heat engines exploiting low-grade thermal reservoirs. The thermal efficiencies of shape-memory-effect heat engines of interest have been estimated from the thermodynamic magnitudes and transformation temperatures of the alloys [1].

The possibility of converting thermal energy into mechanical energy through memory-effect materials has been studied by authors such as Ahlers [2] and Tong et al. [3], who have built various prototypes of solid-state engines with Cu–Zn–Al and Ni–Ti alloys. These prototypes are based on a two-way memory effect in which the material can be made to remember successively and cyclically both, the austenite and

martensite shapes, despite being submitted to up to 70 kg/mm<sup>2</sup> compression stress. This two-way memory effect is achieved through a training process [4–6].

An ideal shape-memory-effect heat-engine cycle has been described in detail elsewhere [3,7]. Ahlers [2], Tong and Wayman [3], Wollants [8] and Verguts et al. [9] have generally agreed that the thermal efficiency for the ideal shape-memory heat-engine cycle can be given as

$$\eta_{\text{th}} = \frac{\Delta H \Delta T_0}{T_0 [C_p \Delta T_0 + \Delta H(\sigma)]} \quad (1)$$

where  $C_p$  is the specific heat of the material and  $\Delta T_0 = T_0(\sigma) - T_0$ ; in which  $T_0$  is the equilibrium temperature. Salzbrenner and Cohen [10] have demonstrated that  $T_0$  is fundamentally indeterminate due to the inseparable elastic and thermal effects. Four stress-dependent transformation temperatures can be measured;  $M_s$  is the initial (austenite→martensite) transformation temperature,  $M_f$  the final transformation temperature,  $A_s$  the initial (martensite→austenite)

\*Corresponding author. Tel.: +34-93-401-6708; fax: +34-93-401-6706; e-mail: gil @cmem.upc.es

reverse transformation temperature and  $A_f$  the final reverse transformation temperature. The temperature  $T_0$  can be approximated as

$$T_0 = 1/2(M_s + A_s) \quad (2)$$

the temperature  $T_0(\sigma)$  can be approximated as:

$$T_0(\sigma) = 1/2(M_s^{\sigma \rightarrow 0} + A_s^{\sigma \rightarrow 0}) \quad (3)$$

being  $M_s^{\sigma \rightarrow 0}$  the initial ( $\beta \rightarrow$  stress induced martensite, SIM) transformation temperature and  $A_s^{\sigma \rightarrow 0}$ , the initial (SIM  $\rightarrow \beta$ ) reverse transformation, both extrapolated to zero stress.

Wollants et al. [8] states that  $\Delta H$  in the denominator of Eq. (1) is a function of stress as given by

$$\Delta H(\sigma) = \frac{\Delta H T_0(\sigma)}{T_0} \quad (4)$$

A comparison of the thermal efficiencies for shape-memory-effect alloy systems can be performed using Eq. (1).

## 2. Materials and experimental method

Five polycrystalline NiTiCu alloys were investigated with chemical compositions shown in Table 1.

For the calorimetric studies, cylindrical test samples 5 mm in diameter, 2 mm high and weighing  $\approx 400$  mg. were submitted to heat treatment (850°C for 10 min and, subsequently, quenched in water at room temperature). The calorimetric measurements were performed twenty-four hours after the heat treatment.

The flow calorimeter used is a highly sensitive model with differential signal detectors made up of 32 thermocouples, the working range of which is from  $-150$  to  $100^\circ\text{C}$ . The temperature was measured by the standard Pt-100 probe. All signals were digitised by a multichannel analyser and treated by a computer. The

heating and cooling rates were  $1^\circ\text{C}/\text{min}$ . The uncertainty of the enthalpy and entropy variations is 5% and  $\pm 0.5$  K in temperature values. The transformation temperatures are taken to be the moment at which a sudden rise in the calorimetric curve takes place and when the signal returns to the base line. The heat absorbed or expelled in the transformation is determined by calculating the area within the curve [11–13].

The mechanical tests were carried out 24 h after the heat treatment using an MTS–Adamel machine at different temperatures ( $10^\circ$ ,  $20^\circ$ ,  $30^\circ$ ,  $40^\circ$ ,  $50^\circ$  and  $70^\circ\text{C}$ ). The cross-head speed was 1 mm/s. A submersible extensometer was used in the tensile tests.

## 3. Experimental results and discussion

Table 2 gives the measured martensitic transformation temperatures, the equilibrium temperatures and enthalpies associated with the transformation. Each of the five alloys studied underwent various cooling–heating cycles and no significant variations were observed in the results. This means that the heating and cooling do not affect the structural order in the appearance or disappearance of defects that could alter the transformation temperatures.

Transformation stresses ( $\beta \rightarrow$  SIM) as well as retransformation stresses (SIM  $\rightarrow \beta$ ) were evaluated at different temperatures. Stress values increase linearly when the temperature increases because the  $\beta$ -phase becomes more stable as temperature increases. Such results may be understood by the fact that increasing mechanical energy is needed to overcome thermodynamic stability. The stress–temperature curves for Alloy 1 can be seen in the Fig. 1; for the alloys studied these being linear equations with correlation coefficients greater than 0.97. As an example,

Table 1

Chemical compositions in weight percentage for the different alloys studied

Alloy	Ni/%	Ti/%	Cu/%
1	48.9	45.1	6.0
2	49.1	45.2	5.7
3	49.5	45.0	5.5
4	49.6	45.0	5.4
5	49.9	45.1	5.0

Table 2

Transformation temperatures (in K) and enthalpies (in J/g)

Alloy	$M_s$	$M_f$	$A_s$	$A_f$	$T_0$	$\Delta H^{\beta \rightarrow M}$	$\Delta H^{M \rightarrow \beta}$
1	291.7	275.1	287.0	310.1	289.4	11.69	12.59
2	290.8	274.7	286.8	310.0	288.8	11.58	12.60
3	289.2	275.0	286.2	309.8	287.7	12.00	12.51
4	290.9	274.9	287.3	309.9	289.3	11.37	12.90
5	290.6	275.3	287.2	310.0	288.9	11.43	12.07

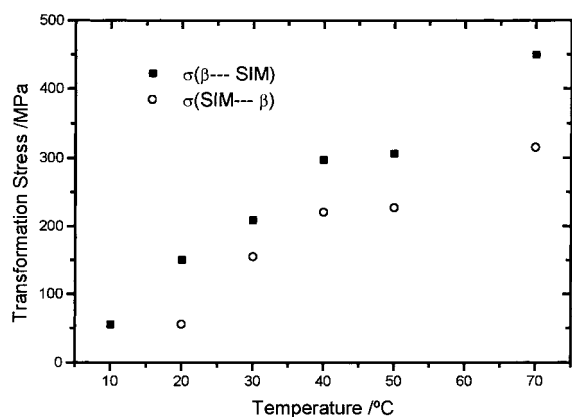


Fig. 1. Transformation stresses vs. test temperatures for Alloy 1.

Table 3

Transformation temperatures determined by calorimetry and by extrapolating the linear equation to the origin, in K

Alloy	$M_s$	$M_s^{\sigma \rightarrow 0}$	$A_s$	$A_s^{\sigma \rightarrow 0}$
1	291.7	262.6	287.0	274.7
2	290.8	261.4	286.8	294.0
3	289.2	292.5	286.2	281.6
4	290.9	271.6	287.3	276.5
5	290.6	262.4	287.2	270.7

Alloy 1 obeys the equation  $\sigma_{\beta \rightarrow \text{SIM}} = -1404.94 + 5.35T$  for the ( $\beta \rightarrow \text{SIM}$ ) transformation and the equation  $\sigma_{\text{SIM} \rightarrow \beta} = -1359.71 + 4.95 \cdot T$  for the ( $\text{SIM} \rightarrow \beta$ ) transformation.

Now,  $M_s^{\sigma \rightarrow 0}$  and  $A_s^{\sigma \rightarrow 0}$  temperatures at zero stress were calculated by extrapolating these linear equations to the origin. Values for each alloy are given in Table 3. Theoretically,  $M_s^{\sigma \rightarrow 0}$  at zero stress and  $M_s$  should be the same value. However, comparing the values of  $M_s$  measured by calorimetry with those extrapolated at zero stress, it can be noticed that, in all cases, the extrapolated values of  $M_s$  are lower. The difference between the  $M_s$  and  $M_s^{\sigma \rightarrow 0}$  temperatures can be accounted for by the fact that the thermal transformation ( $\beta \rightarrow$ martensite) gives rise to several self-accommodating martensitic variants. Therefore, less energy than an SIM transformation is required where only a few preferred variants are formed. Moreover, the SIM transformation ( $\beta \rightarrow \text{SIM}$ ) takes place by applying a stress which produces more defects than quenching. These defects will inhibit plate growth.

Table 4

Equilibrium temperatures and enthalpies associated with SIM transformation

Alloy	$T_0(\sigma)/\text{K}$	$\Delta H(\sigma)/(\text{J/g})$
1	268.7	11.3
2	277.7	11.6
3	287.1	12.3
4	274.0	11.5
5	266.5	10.9

In fact,  $M_s^{\sigma \rightarrow 0}$  temperatures should be lower than the calorimetrically measured  $M_s$  ones, due to the different sensitivities of the experimental techniques. It has been noticed that when the start of the transformation is detected calorimetrically, there are still no changes in the stress–strain curve.

The equilibrium temperature under stress  $T_0(\sigma)$  is calculated from Eq. (3) and the enthalpy associated with SIM transformation from Eq. (4). These values are shown in Table 4. The SIM transformation enthalpies are always higher than those originating thermally. This variation can be explained in the same terms as for the  $M_s$  temperatures. More heat is needed in order to produce SIM.

Thermal efficiencies calculated from Eq. (1) and Carnot efficiencies calculated by the ratio of the integration of thermograms between the transforma-

Table 5

Thermal and Carnot efficiencies

Alloy	$\eta_{\text{th}}$	$\eta_{\text{Car}}$	Reference
NiTiCu 1	5.1	24.9	
NiTiCu 2	5.4	25.0	
NiTiCu 3	5.0	24.3	
NiTiCu 4	4.8	24.2	
NiTiCu 5	5.3	23.6	
49.8Ni–Ti	3.4	16.4	[17]
51.6Ni–Ti	3.2	14.9	[17]
50.6Ni–Ti	3.2	13.6	[17]
Cu–27.6Al–3.8Ni	4.2	42.4	[18]
Cu–25.3Zn–9.1Al	5.2	31.9	[19]
Cu–16.1Zn–16.0Al	4.9	28.6	[8]
Au–29Cu–45Zn	1.4	15.6	[14]
Au–28Cu–46Zn	1.5	9.0	[14]
Au–47.5Ag–47.5Cd	1.8	22.0	[15]
Au–47.5Cd	3.5	—	[15]
Ag–45Cd	5.0	31.9	[15]
In–21Tl	0.1	—	[16]
In–26Tl	0.6	—	[16]

tion temperatures (heat exchanged in the cooling or heating cycles) and the reversible work produced by the thermoelastic martensitic transformation are presented in Table 5.  $C_p$  values were calculated from Neumann–Kopp rule, after assuming that the Debye temperature of the alloy was below  $M_s$ , in these alloys  $C_p$  was 0.55 J/gK. These efficiencies have been obtained for other shape-memory alloys, Miura et al. [14,15] established that the thermal efficiency in In–Ti ranges from 0.12 to 0.50%, and for Au–Ag–Cd it ranges between 1.2 and 2.0% [16]. In the case of Ag–Cd [17], the values are very similar to those for NiTiCu alloys, ranging from five to 5.5%. The addition of Cu in NiTi produces an increase of around 60% in thermal efficiency and from 15% to 25% in the Carnot efficiency. This is a significant increase as can be seen from Table 5.

#### 4. Conclusions

The addition of Cu (5–6% in weight percentage) in NiTi produced an increase in the thermal and the Carnot efficiencies. Small changes of the chemical composition of NiTiCu alloys did not affect their martensitic transformation characteristics in comparison with other shape-memory alloys. This stability produces an increase in the stability and reproducibility of the properties of these alloys producing an important improvement to design new shape-memory effect heat engines.

#### References

- [1] A.P. Jardine, *J. Mat. Sci.* 24 (1998) 2587.
- [2] M. Ahlers, *Scripta Met.* 9 (1975) 7174.
- [3] C.M. Wayman, H.C. Tong, *Acta Met.* 22 (1974) 887.
- [4] K. Shimizu, T. Tadaki, in Funakubo (Ed.), *Shape Memory Alloys*, Gordon and Breach Science Publishers, Tokyo, 1986, p. 19.
- [5] R.V. Krishnan, L. Delaey, H. Tas, H. Warlimont, *J. Mater. Sci.* 9 (1974) 1536.
- [6] T.A. Schroeder, I. Cornelisy, C.M. Wayman, *Metall. Trans. A* 7A (1976) 535–546.
- [7] C.M. Wayman, H.C. Tong, *Scripta Metall.* 11 (1977) 341.
- [8] P. Wollants, M. De Bonte, J. Roos, *Z. Metallkde* 70 (1979) 113.
- [9] H. Verguts, E. Aernoudt, W. Vermeersch, *J. De Physique, Colloque C4*, 43(12) (1982) 825.
- [10] R.J. Salzbrenner, M. Cohen, *Acta Metall.* 24 (1980) 739.
- [11] J.M. Guilemany, F.J. Gil, *J. Mater. Sci.* 26 (1991) 4626.
- [12] F.J. Gil, *Tesis Doctoral*, Universidad de Barcelona, 1989.
- [13] J. Muntasell, J.L. Tamarit, E. Cesari, J.M. Guilemany, F.J. Gil, *Mater. Res. Bull.* 24 (1989) 445.
- [14] S. Miura, S. Maeda, N. Nakanishi, *Phil. Mag.* 30 (1974) 565.
- [15] S. Miura, F. Hori, N. Nakanishi, *Phil. Mag.* 40 (1979) 661.
- [16] S. Miura, M. Ito, K. Endo, N. Nakanishi, *Mem. Fac. Eng. Kyoto Univ.* 43 (1983) 287.
- [17] S. Miyazaki, Y. Ohmi, K. Otsuka, Y. Suzuki, *Proc. ICOMAT (Leuven) J. de Phys.* 12(43) (1982) C4–255.
- [18] K. Otsuka, H. Sakamoto, K. Shimizu, *Acta Metall.* 27 (1979) 585.
- [19] T. Saburi, Y. Inada, S. Nenno, N. Hori, *Proc. ICOMAT (Leuven) J. de Phys.* 12(43) (1982) C4–633.